Temporal and Spatial Variations of NO_x and Ozone Concentrations in Seoul during the Solar Eclipse of 22 July 2009

KYUNG-HWAN KWAK, YOUNG-HEE RYU, AND JONG-JIN BAIK

School of Earth and Environmental Sciences, Seoul National University, Seoul, South Korea

(Manuscript received 20 May 2010, in final form 19 October 2010)

ABSTRACT

The temporal and spatial variations of NO, NO_2, and O_3 concentrations in Seoul, South Korea, during the solar eclipse of 22 July 2009 are investigated by analyzing data measured at 25 environmental monitoring stations. The NO_2 concentration increases and the NO and O_3 concentrations decrease because the efficiency of NO_2 photolysis decreases during the solar eclipse. About an hour after the maximum obscuration, the reduction in the average O_3 concentration over Seoul is estimated to be 45%. The maximum reduction in the O_3 concentration downwind of the NO_x source area is higher and occurs later than that in the downtown region. Deviations from the NO–NO_2–O_3 photostationary state in the downwind region are larger than those in the downtown region. This result implies that, in addition to the photochemical effect, the effect of transport by winds increases the reduction potential of the O_3 concentration in the downwind region during the solar eclipse.

1. Introduction

Direct emissions of primary pollutants such as nitrogen oxides (NO_x) and volatile organic compounds have increased in most megacities. Ozone (O_3), a secondary pollutant formed by photochemical reactions involving primary pollutants (i.e., precursors), has accordingly received considerable attention. Because photochemical reactions occur in the presence of sunlight, it is very important to understand the effect of changes in solar radiation on the concentrations of O_3 and its precursors. Aerosols also interact with solar radiation and hence influence radiative forcing. Many observational studies have investigated the diurnal variation of pollutant concentrations (Mayer 1999; Trainer et al. 2000; Lal et al. 2000; Kanaya et al. 2007) as well as the seasonal variation of aerosol forcing (Tzanis and Varotsos 2008) associated with changes in solar radiation.

Because NO_x and O_3 are sensitive to changes in solar radiation, it is difficult to fully understand their characteristics in the atmosphere, even by examining their overall diurnal variations. A solar eclipse provides a great opportunity to study the characteristics of photochemical pollutants because there is a sharp decrease in solar radiation over a large area for a relatively short time period. The impacts of a solar eclipse on photochemical pollutant concentrations have been investigated (Eastman and Stedman 1980; Abram et al. 2000; Zanis et al. 2001, 2007; Tzanis et al. 2008). Tzanis et al. (2008) examined the behavior of surface O_3 concentration in Athens, Greece, during the solar eclipse of 29 March 2006. They observed that the maximum reduction in surface O_3 concentration occurred 1 h after the maximum obscuration in Athens.

In this study, we investigate the temporal and spatial variations of NO_x and O_3 concentrations associated with a dramatic change in solar radiation in Seoul, South Korea, during the solar eclipse of 22 July 2009. Environmental monitoring stations in Seoul are densely spaced, thus enabling us to examine the spatial variation of any measured pollutant concentration within the megacity. This is a salient aspect of this study.

2. Observation data

In Seoul (37.5°N, 127.0°E), the solar eclipse of 22 July 2009 started at 0934 LT, reached the maximum obscuration (78.5%) at 1048 LT, and ended at 1205 LT. The cloud cover was $^3/_{10}$–$^4/_{10}$. Figure 1 shows the diurnal variations of the hourly averaged global solar radiation and 10-min-averaged air temperature at Seoul

Corresponding author address: Jong-Jin Baik, School of Earth and Environmental Sciences, Seoul National University, Seoul 151-742, South Korea.
E-mail: jjbaik@snu.ac.kr

DOI: 10.1175/2010JAMC2561.1

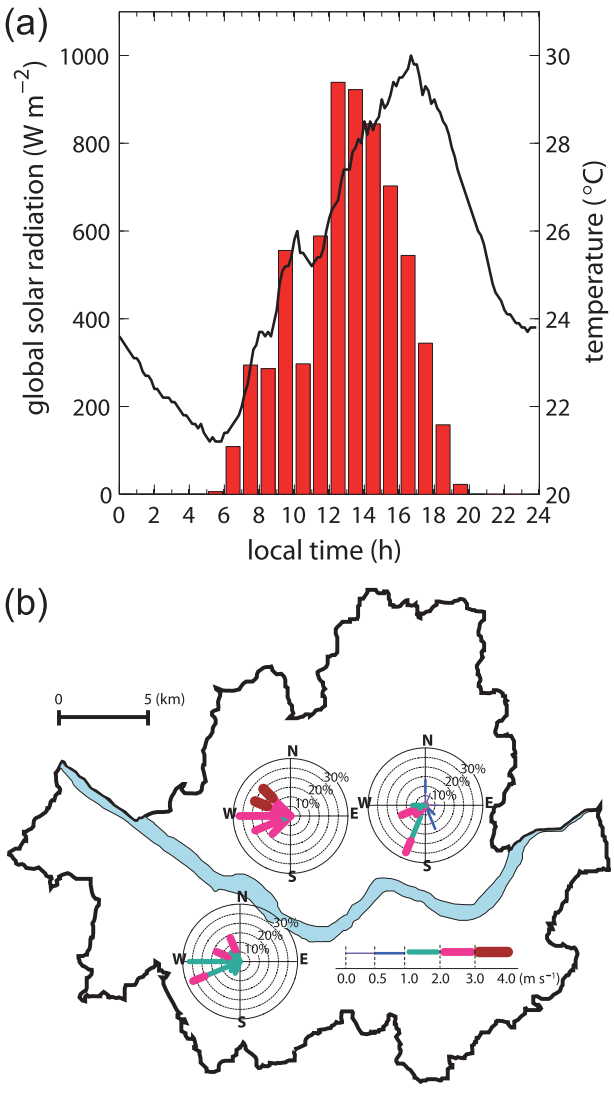

FIG. 1. (a) Time series of hourly averaged global solar radiation (bars) and 10-min-averaged air temperature (solid line) at 1.5 m on 22 Jul 2009, and (b) wind roses at the northwest, northeast, and southwest stations during the solar eclipse. Seoul Meteorological Observatory is the northwest station.

Meteorological Observatory on 22 July 2009. The hourly averaged global solar radiation was significantly reduced between 1000 and 1100 LT, and the air temperature decreased by 0.8°C from 26.0°C (at 1010 LT) to 25.2°C (at 1100 LT). The wind speed and wind direction at three automatic weather stations are analyzed during the solar eclipse (Fig. 1). The predominant wind was westerly at the northwest and southwest stations and south-southwesterly at the northeast station. The wind speed was relatively low, ranging from 1 to 3 m s^{-1}.

The NO, NO_2, and O_3 concentrations—hereinafter denoted by [NO], [NO_2], and [O_3], respectively—were measured at 25 environmental monitoring stations in Seoul. The hourly averaged observation data were provided by the Seoul Metropolitan Government Research Institute of Public Health and Environment. Equipment used to measure pollutant concentrations are NA-623 (Kimoto Electric Co., Ltd.), APMA-370 (Horiba, Ltd.), AC31M (Environnement S.A.), and EC9841 (American Ecotech Co.) chemiluminescence NO_x analyzers and OA-681 (Kimoto), APOA-370 (Horiba), O341M (Environnement S.A.), and EC9810 (American Ecotech) UV absorption O_3 analyzers. Note that the equipment types used to measure NO_x or O_3 concentration at the environmental monitoring stations in Seoul are not the same. Following installation and management guidelines on environmental monitoring stations distributed by the Korea Ministry of Environment, the concentrations given in parts per billion (ppb) are rounded off to the nearest whole number. Abnormal data are automatically screened out (see http://www.airkorea.or.kr/airkorea/eng/index.jsp). Following the data screening, some missed or erroneous data from three stations are excluded when calculating the spatial average. The time represented in data indicates the end of the averaging period. Most of the environmental monitoring stations are located on rooftops of two- or three-story buildings where there is no severe source of pollutants within tens of meters. In addition to the 25 stations, data from five roadside environmental monitoring stations are used to identify the characteristics of NO_x sources.

3. Results and discussion

The diurnal variations of [NO], [NO_2], and [O_3] can change during a solar eclipse. Figure 2a shows the diurnal variations of [NO], [NO_2], and [O_3] in Seoul on the day of the solar eclipse. Before the solar eclipse, in the rush hour, massively emitted NO is converted to NO_2, thus maintaining high [NO_2]. During the solar eclipse (shaded part in Fig. 2), the trends in the concentrations of the three species deviate from the usual daily trends in which [NO_x] decreases and [O_3] increases in the late morning. While NO titration of O_3 still works, the reduction in solar radiation decreases the efficiency of NO_2 photolysis. As a result, [NO_2] increases but [NO] and [O_3] decrease. After the solar eclipse, in the early afternoon, the trends in the concentrations of the three species return to their usual trends in the absence of a solar eclipse.

To quantify the decrease in [O_3] due to a solar eclipse, it is necessary to estimate [O_3] in the absence of a solar eclipse. The [O_3] would be higher in the absence of a solar eclipse relative to the value in the presence of a solar eclipse. Zanis et al. (2001) calculated the decrease in [O_3]

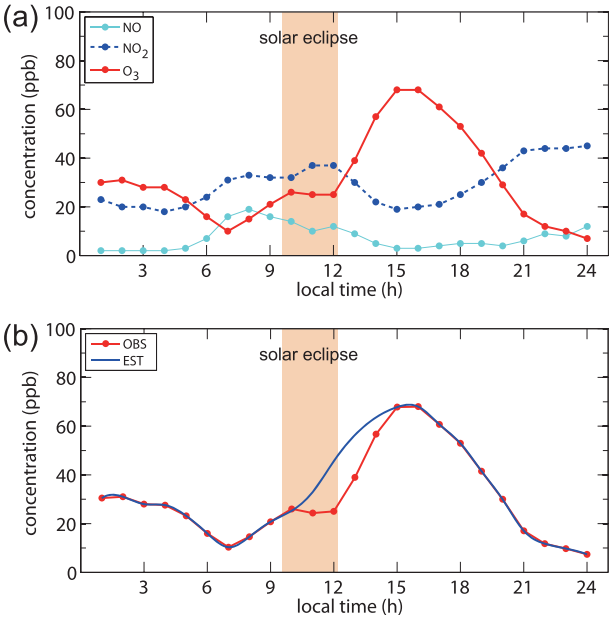

FIG. 2. Time series of (a) [NO], [NO_2], and [O_3] and (b) the observed (OBS) and estimated (EST) [O_3]. All concentrations are averaged over Seoul.

due to a solar eclipse by using a photochemical box model. Tzanis et al. (2008) fitted expected [O_3] curves using [O_3] measurement data obtained in the absence of a solar eclipse. Then, they estimated the decrease in [O_3] due to the solar eclipse. An approach used to quantify the decrease in [O_3] due to the solar eclipse in this study is different from the approaches of Zanis et al. (2001) and Tzanis et al. (2008). In the two previous studies, the maximum obscurations were observed in the afternoon. On the other hand, in the case of the solar eclipse of 22 July 2009 in Seoul, the maximum obscuration was observed in the morning. In general, [O_3] increases in the morning in the absence of a solar eclipse. To estimate [O_3], the O_3 production rate ($\Delta[O_3]/\Delta t$) in the absence of the solar eclipse is calculated using [O_3] data for days on which there were no eclipses. Selected days were 23 July 2004, 21 July 2005, and 4 August 2009. The conditions on these days were similar to those on the eclipse day in terms of season, day of the week, cloud cover, wind direction, and [NO_2] in the early morning. It is assumed that [O_3] before the beginning of the solar eclipse (0934 LT) and after the period including the daily [O_3] maximum (1500–1600 LT) is not affected by the solar eclipse. Then, [O_3] excluding the effect of the solar eclipse is estimated by integrating the O_3 production rate in time from the beginning of the solar eclipse to its end. After the estimated [O_3] is obtained for the period up to 1200 LT, a spline interpolation method is employed to estimate [O_3] at 1300 and 1400 LT. This method is found to reproduce

TABLE 1. Observed [O_3] (OBS), differences (DIF) between the estimated (EST) and observed [O_3], and the ratios DIF/EST from 1000 to 1400 LT.

Local time (h)	OBS (ppb)	DIF (ppb)	DIF/EST
1000	26.0	−0.8	−0.03
1100	24.3	8.7	0.26
1200	25.0	20.6	0.45
1300	39.0	17.4	0.31
1400	56.7	6.9	0.11

the temporal variation of [O_3] from 1200 to 1500 LT considerably well.

Figure 2b shows the diurnal variations of the observed [O_3] and the estimated [O_3]. As expected, the estimated [O_3] that excludes the effect of the solar eclipse steadily increases in the morning. Table 1 lists the [O_3] reduction and the ratio of the [O_3] reduction to the estimated [O_3] ([O_3] reduction ratio) at 1000, 1100, 1200, 1300, and 1400 LT. Hereinafter, the [O_3] reduction is defined as the difference between the estimated [O_3] and the observed [O_3]. The [O_3] reduction reaches a maximum at 1200 LT (20.6 ppb), with an [O_3] reduction ratio of 0.45. The maximum [O_3] reduction is observed about an hour after the maximum obscuration. This result is consistent with that of Tzanis et al. (2008). After the end of the solar eclipse, [O_3] does not immediately recover to the estimated [O_3]. This indicates that the effect of the solar eclipse on [O_3] continues for at least 2 h.

The [O_3] varies spatially within a city because [O_3] is influenced not only by the solar eclipse but also by local NO_x emission and meteorological factors. In Seoul, NO_x is largely emitted in downtown regions and industrial complexes and is transported to downwind regions (Kim and Ghim 2002). Because downtown regions are located in the central area of Seoul and many industrial pollutant source regions are located in the western area of Seoul, prevailing westerly winds transport O_3 and its precursors to the eastern area of Seoul (Chung and Chung 1991). Wind channeling in the Han River valley and blocking of air pollutants due to several mountains produce multiple regions of high [O_3] in Seoul (Chung and Chung 1991). Oh et al. (2005) investigated the typical patterns of surface [O_3] and their dependence on meteorological factors during high [O_3] events (118 days) from 1998 to 2002. They found that the inland penetration of sea breezes interacting with synoptic flows is one of the key factors determining the spatial variation of [O_3] in Seoul.

To characterize the spatial variation of [O_3], Seoul is divided into four regions: hillside (HS), downtown (DT), northeast (NE), and southwest (SW) regions (see Fig. 3). The DT region is characterized as a heavy-traffic region

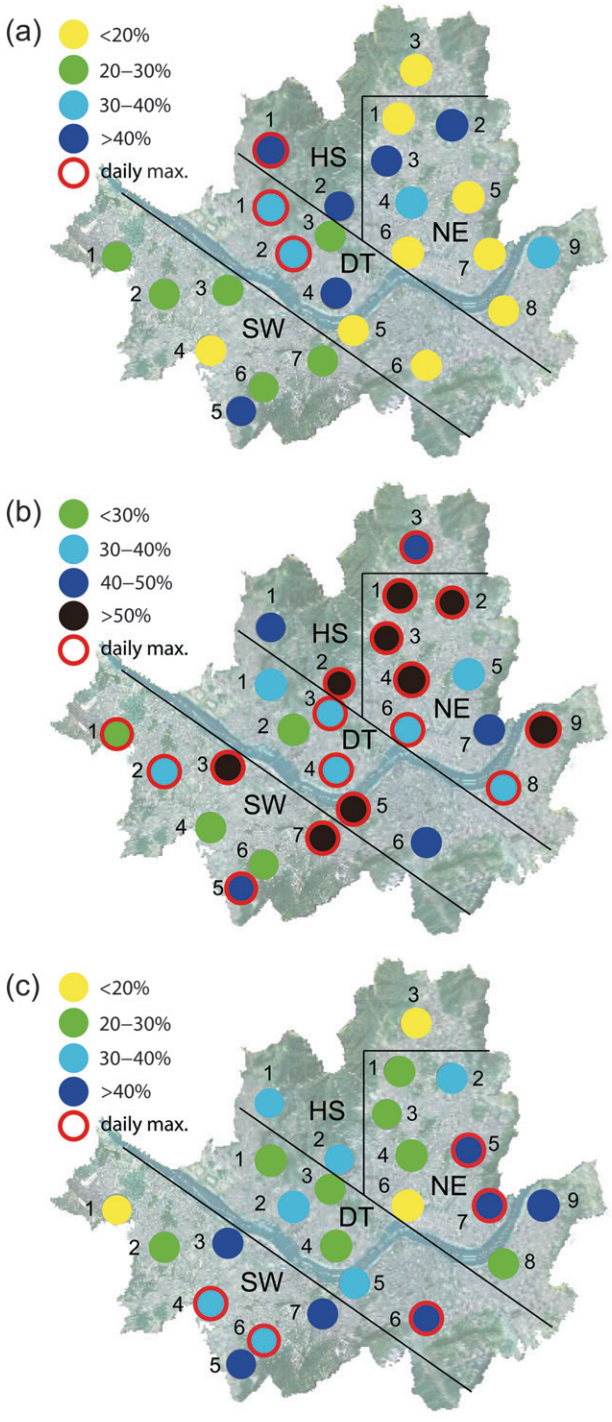

FIG. 3. Spatial distributions of the [O_3] reduction ratio at (a) 1100, (b) 1200, and (c) 1300 LT. Outer rings indicate the daily maximum [O_3] reduction ratio for each station. The 25 stations are divided into four groups: HS (1–3), DT (1–6), NE (1–9), and SW (1–7) regions, as defined in the text.

TABLE 2. Average [NO], [NO_2], and [O_3] (ppb) for each group from 1100 to 1300 LT. Each group comprises the stations at which the daily maximum [O_3] reduction ratio is observed at the same local time. The stations in group 1100 LT, group 1200 LT, and group 1300 LT are indicated by outer rings in Figs. 3a, 3b, and 3c, respectively.

Local	Group 1100 LT			Group 1200 LT			Group 1300 LT		
time (h)	[NO]	[NO_2]	[O_3]	[NO]	[NO_2]	[O_3]	[NO]	[NO_2]	[O_3]
1100	15	42	17	9	36	26	10	38	27
1200	10	28	27	13	38	24	11	37	28
1300	7	21	38	8	28	41	14	42	33

with high NO_x emission in the rush hour. Because the predominant wind is westerly to south-southwesterly, the NE region is characterized as a downwind region relative to the DT region. Some industrial complexes are located in the SW region and other industrial complexes are located farther westward outside Seoul (Lee et al. 2008). These industrial complexes act as pollutant sources. Therefore, the SW region is characterized as a downwind region relative to the industrial complexes outside Seoul as well as a source region. The HS region includes a mountain region in northern Seoul, which exhibits slightly different features of pollutant concentrations.

Figure 3 shows the spatial distributions of the [O_3] reduction ratio in percentage ([O_3] reduction/estimated [O_3] $\times$ 100). At 1100 LT, the [O_3] reduction ratio is relatively small in the NE and SW regions (Fig. 3a). It is the largest at HS-2 (station 2 in the HS region) and is over 30% at 10 stations. At this time, the daily maximum [O_3] reduction ratio is shown at HS-1, DT-1, and DT-2. Group 1100 LT in Table 2 comprises the three stations. At 1200 LT, the increase in the [O_3] reduction ratio from 1100 to 1200 LT is significant, especially in the northern part of the NE region downwind of the central business district located near DT-3 (Fig. 3b). Out of 25 stations, 21—including HS-2 (61%), NE-2 (63%), NE-3 (63%), and NE-9 (62%)—show an [O_3] reduction ratio of over 30%. At this time, 17 stations (group 1200 LT in Table 2) show the daily maximum [O_3] reduction ratio. At 1300 LT, after the end of the solar eclipse, the effect of the solar eclipse on [O_3] is still observed (Fig. 3c). In contrast to 1100 and 1200 LT, the [O_3] reduction ratio is relatively large in the eastern and southern parts of Seoul at 1300 LT. Fourteen stations show an [O_3] reduction ratio of over 30%, including the highest ratio at SW-6 (53%). The daily maximum [O_3] reduction ratio is shown at DT-6, NE-5, NE-7, SW-4, and SW-6 (group 1300 LT in Table 2).

Table 2 lists the average [NO], [NO_2], and [O_3] for each group defined in Fig. 3 at 1100, 1200, and 1300 LT. At

1100 LT, for example, the lowest $[O_3]$ among these three groups is 17 ppb in group 1100 LT—this is associated with the highest [NO] of 15 ppb and $[NO_2]$ of 42 ppb in the same group. This association is also observed in group 1200 LT at 1200 LT and group 1300 LT at 1300 LT. Note that the stations in group 1100 LT have less inflow of polluted air and that those in groups 1200 LT and 1300 LT are mostly located in near- and far-downwind regions, respectively. The region of the daily maximum $[O_3]$ reduction ratio tends to be shifted from the upwind region to the downwind region with time (Fig. 3). The results listed in Table 2 imply that during and even after the end of the solar eclipse O_3 formation is strongly suppressed by the presence of abundant NO_x that originates from the major source regions and is transported to the downwind regions.

We examine deviations in [NO], $[NO_2]$, and $[O_3]$ from the NO–NO_2–O_3 photostationary state (PSS) of the following chemical reactions (Carpenter et al. 1998):

$$NO_2 \xrightarrow{h\nu} NO + O(^3P), \tag{1}$$

$$O(^3P) + O_2 + M \rightarrow O_3 + M, \quad \text{and} \tag{2}$$

$$NO + O_3 \rightarrow NO_2 + O_2. \tag{3}$$

From the above chemical reactions, we obtain the relationship

$$\frac{J_{NO2}}{k_3} = \frac{[O_3]}{[NO_2]/[NO]}, \tag{4}$$

where J_{NO2} is the photolysis rate and k_3 is the reaction rate constant of Eq. (3). In this study, J_{NO2} is calculated using an empirical method (Schere and Demerjian 1978; Wiegand and Bofinger 2000). This method, validated using data from a radiative transfer model, uses global solar radiation (GSR; W m^{-2}) and solar zenith angle χ to calculate J_{NO2} (min^{-1}):

$$J_{NO2} = \begin{cases} \text{GSR} \times \left[(4.23 \times 10^{-4}) + 1.09 \times \dfrac{10^{-4}}{\cos\chi}\right] & \text{for} \quad 0^\circ \le \chi < 47^\circ, \\ \text{GSR} \times (5.82 \times 10^{-4}) & \text{for} \quad 47^\circ \le \chi < 64^\circ, \quad \text{and} \\ \text{GSR} \times [(-0.997 \times 10^{-4}) + (1.2 \times 10^{-3})(1 - \cos\chi)] & \text{for} \quad 64^\circ \le \chi < 90^\circ. \end{cases} \tag{5}$$

From the global solar radiation shown in Fig. 1a, J_{NO2} is 5.29×10^{-3} s^{-1} at 1000 LT, 2.73×10^{-3} s^{-1} at 1100 LT, 5.30×10^{-3} s^{-1} at 1200 LT, and 8.40×10^{-3} s^{-1} at 1300 LT; therefore, the J_{NO2}/k_3 ratio is 11.75 ppb at 1000 LT, 6.11 ppb at 1100 LT, 11.68 ppb at 1200 LT, and 18.20 ppb at 1300 LT. At 1300 LT, when there was a clear sky with a cloud cover of 2/10, the global solar radiation was the largest of the day. The J_{NO2} value of 8.40×10^{-3} s^{-1} is comparable to 8.14×10^{-3} s^{-1} in Seinfeld and Pandis (2006) and the value after the solar eclipse in Zanis et al. (2001).

Deviations in $[O_3]$ from the NO–NO_2–O_3 PSS can be caused by NO_x emission, the enhancement of peroxy radicals (e.g., HO_2 and RO_2), and rapid changes in solar radiation (Matsumoto et al. 2006). The effect of peroxy radicals is relatively insignificant during a solar eclipse because their levels are suppressed by the reduction in actinic flux (Zanis et al. 2007). As indicated by Zanis et al. (2001), deviations in $[O_3]$ from the NO–NO_2–O_3 PSS can also be caused by transport from nearby polluted areas.

To confirm the implication from Fig. 3 and Table 2 showing large $[O_3]$ reduction along with abundant NO_x, we examine deviations of the observed concentration ratio $[O_3]/([NO_2]/[NO])$ from J_{NO2}/k_3 in the four regions. In the ideal, in the NO–NO_2–O_3 PSS that takes only a photochemical effect into account, the observed concentration ratio $[O_3]/([NO_2]/[NO])$ is equivalent to a well-estimated J_{NO2}/k_3 that decreases from 1000 to 1100 LT and turns to increase from 1100 to 1200 LT. Figure 4 shows diagrams of $[O_3]$ and $[NO_2]/[NO]$ averaged over each region from 0800 to 1400 LT. In the four regions, except a roadside region, $[NO_2]/[NO]$ increases from 1000 to 1100 LT and decreases from 1100 to 1200 LT. From 1000 to 1200 LT, $[O_3]$ increases in the DT region (Fig. 4a) but decreases in the NE region (Fig. 4b). In the HS and SW regions, $[O_3]$ decreases from 1000 to 1100 LT and turns to increase from 1100 to 1200 LT (Fig. 4c). The most distinctive feature between the NE and DT regions is the $[NO_2]/[NO]$ ratio. This ratio is larger than 3 in the NE region but smaller than 3 in the DT region between 1100 and 1300 LT. Regional differences in $[O_3]$ and $[NO_2]/[NO]$ lead to differences in deviations from the NO–NO_2–O_3 PSS. The deviations at 1200 and 1300 LT are small in the DT region but large in the NE region. Because $[NO_2]/[NO]$ is small for freshly emitted pollutants but large for transported pollutants, the regional differences could be attributed to NO_x emission and transport. Note that in the roadside region, which has an extreme condition of the DT region ($[NO_2]/[NO]$ is less than 1), large deviations from the PSS do not appear

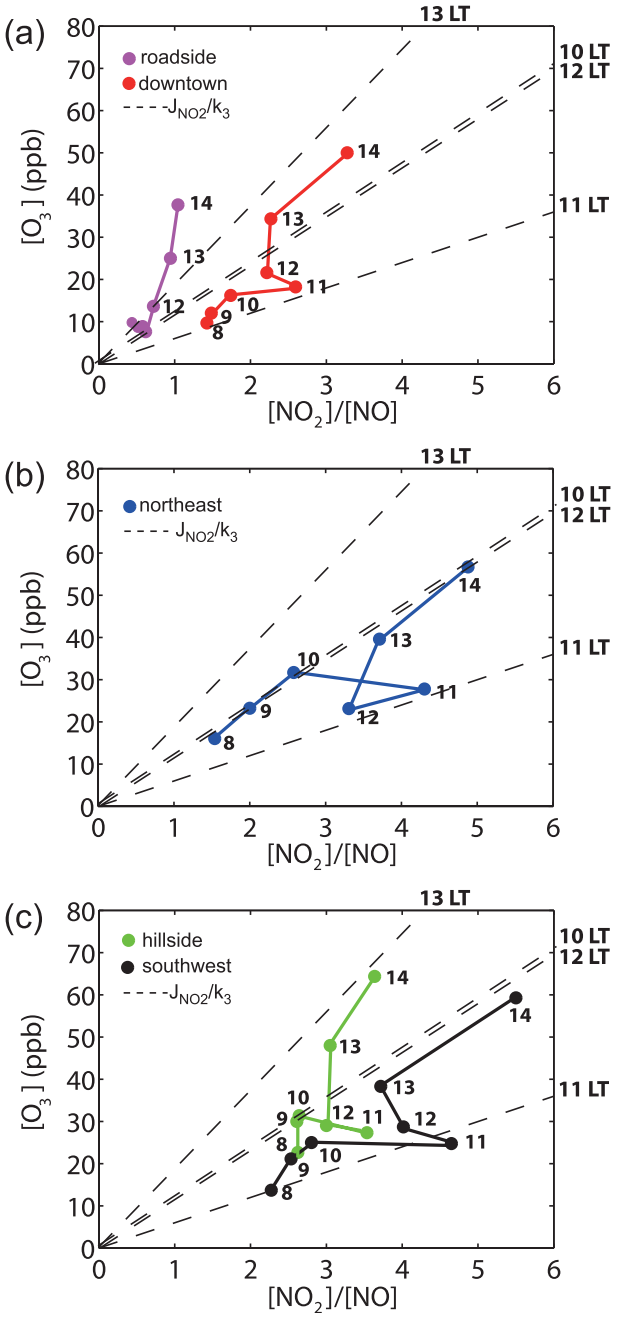

FIG. 4. Diagrams of $[O_3]$ and $[NO_2]/[NO]$ averaged over each region from 0800 to 1400 LT. The numbers denote local time. The NO–NO_2–O_3 PSSs at 1000, 1100, 1200, and 1300 LT are indicated by dashed lines.

during the solar eclipse. NO_x transport from source areas is largely responsible for the large $[O_3]$ reduction as well as the large $[NO_2]/[NO]$ in the NE region even after the end of the solar eclipse. This is confirmed by the large deviations from the NO–NO_2–O_3 PSS in the NE region. As a consequence, apart from the photochemical effect on [NO], $[NO_2]$, and $[O_3]$, the transport effect greatly influences the spatial distributions of [NO], $[NO_2]$, and $[O_3]$ in Seoul. This is consistent with the implication from Fig. 3 and Table 2.

4. Conclusions

The temporal and spatial variations of NO_x and O_3 in Seoul during the solar eclipse of 22 July 2009 were examined. The results showed that the $[O_3]$ reduction ratio is 0.45 on average about an hour after the maximum obscuration and that the region of large $[O_3]$ reduction tends to be extended toward the downwind region with time. In the downtown region, the $[O_3]$ reduction ratio is relatively small, although previous studies showed that an $[O_3]$ reduction due to a solar eclipse is large in urban areas. In the downwind region, on the other hand, the $[O_3]$ reduction ratio as well as $[NO_2]/[NO]$ are larger than those in the downtown region. Deviations from the NO–NO_2–O_3 PSS in the downwind region are also larger than those in the downtown region. From regional differences in the $[O_3]$ reduction ratio and deviations from the PSS, it was found that the effect of the solar eclipse on $[O_3]$ is spatially inhomogeneous even on a scale of tens of kilometers. During the solar eclipse, NO_x transport by winds is the most possible reason for the spatial variation of the $[O_3]$ reduction. A modeling study is needed to quantify the effects of NO_x transport by winds as well as geographical and other meteorological factors on the $[O_3]$ reduction during the solar eclipse.

Acknowledgments. The authors are grateful to two anonymous reviewers for providing valuable comments that led to the improvements of the original manuscript. This work was funded by the Korea Meteorological Administration Research and Development Program under Grant RACS 2010-4005 and by the Brain Korea 21 Project.

REFERENCES

Abram, J. P., D. J. Creasey, D. E. Heard, J. D. Lee, and M. J. Pilling, 2000: Hydroxyl radical and ozone measurements in England during the solar eclipse of 11 August 1999. *Geophys. Res. Lett.,* **27,** 3437–3440.

Carpenter, L. J., K. C. Clemitshaw, R. A. Burgess, S. A. Penkett, J. N. Cape, and G. G. McFadyen, 1998: Investigation and evaluation of the NO_x/O_3 photochemical steady state. *Atmos. Environ.,* **32,** 3353–3365.

Chung, Y.-S., and J.-S. Chung, 1991: On surface ozone observed in the Seoul metropolitan area during 1989 and 1990 (in Korean). *J. Korea Air Pollut. Res. Assoc.,* **7,** 169–179.

Eastman, J. A., and D. H. Stedman, 1980: Variations in the ambient ozone concentration during the 26 February 1979 solar eclipse. *Atmos. Environ.,* **14,** 731–732.

Kanaya, Y., and Coauthors, 2007: Diurnal variations in H_2O_2, O_3, PAN, HNO_3 and aldehyde concentrations and NO/NO_2 ratios at Rishiri Island, Japan: Potential influence from iodine chemistry. *Sci. Total Environ.,* **376,** 185–197.

Kim, J. Y., and Y. S. Ghim, 2002: Effects of the density of meteorological observations on the diagnostic wind fields and the performance of photochemical modeling in the greater Seoul area. *Atmos. Environ.,* **36,** 201–212.

Lal, S., M. Naja, and B. H. Subbaraya, 2000: Seasonal variations in surface ozone and its precursors over an urban site in India. *Atmos. Environ.,* **34,** 2713–2724.

Lee, M., J.-A. Kim, Y.-M. Kim, and G. Lee, 2008: Characteristics of atmospheric hydrogen peroxide variations in Seoul megacity during 2002–2004. *Sci. Total Environ.,* **393,** 299–308.

Matsumoto, J., N. Kosugi, A. Nishiyama, R. Isozaki, Y. Sadanaga, S. Kato, H. Bandow, and Y. Kajii, 2006: Examination on photostationary state of NO_x in the urban atmosphere in Japan. *Atmos. Environ.,* **40,** 3230–3239.

Mayer, H., 1999: Air pollution in cities. *Atmos. Environ.,* **33,** 4029–4037.

Oh, I.-B., Y.-K. Kim, and M.-K. Hwang, 2005: Ozone pollution patterns and the relation to meteorological conditions in the greater Seoul area (in Korean). *J. Korean Soc. Atmos. Environ.,* **21,** 357–365.

Schere, K. L., and K. L. Demerjian, 1978: A photochemical box model for urban air quality simulation. Preprints, *Fourth Joint Conf. on Sensing of Environmental Pollutants,* New Orleans, LA, Amer. Chem. Soc., 427–433.

Seinfeld, J. H., and S. N. Pandis, 2006: *Atmospheric Chemistry and Physics: From Air Pollution to Climate Change*. 2nd ed. John Wiley and Sons, 1203 pp.

Trainer, M., D. D. Parrish, P. D. Goldan, J. Roberts, and F. C. Fehsenfeld, 2000: Review of observation-based analysis of the regional factors influencing ozone concentrations. *Atmos. Environ.,* **34,** 2045–2061.

Tzanis, C., and C. A. Varotsos, 2008: Tropospheric aerosol forcing of climate: A case study for the greater area of Greece. *Int. J. Remote Sens.,* **29,** 2507–2517.

——, ——, and L. Viras, 2008: Impacts of the solar eclipse of 29 March 2006 on the surface ozone concentration, the solar ultraviolet radiation and the meteorological parameters at Athens, Greece. *Atmos. Chem. Phys.,* **8,** 425–430.

Wiegand, A. N., and N. D. Bofinger, 2000: Review of empirical methods for the calculation of the diurnal NO_2 photolysis rate coefficient. *Atmos. Environ.,* **34,** 99–108.

Zanis, P., and Coauthors, 2001: Comparison of measured and modeled surface ozone concentrations at two different sites in Europe during the solar eclipse on August 11, 1999. *Atmos. Environ.,* **35,** 4663–4673.

——, and Coauthors, 2007: Effects on surface atmospheric photooxidants over Greece during the total solar eclipse event of 29 March 2006. *Atmos. Chem. Phys.,* **7,** 6061–6073.